J Neurophysiol 109: 1525–1534, 2013.
First published January 2, 2013; doi:10.1152/jn.00924.2012.

Olivocochlear suppression of outer hair cells in vivo: evidence for combined action of BK and SK2 channels throughout the cochlea

Stéphane F. Maison,[1,2,3] Sonja J. Pyott,[4] Andrea L. Meredith,[5] and M. Charles Liberman[1,2,3]

[1]*Department of Otology and Laryngology, Harvard Medical School, Boston, Massachusetts;* [2]*Eaton-Peabody Laboratory, Massachusetts Eye and Ear Infirmary, Boston, Massachusetts;* [3]*Harvard Program in Speech and Hearing Bioscience and Technology, Boston, Massachusetts;* [4]*Department of Biology and Marine Biology, University of North Carolina Wilmington, Wilmington, North Carolina; and* [5]*Department of Physiology, University of Maryland School of Medicine, Baltimore, Maryland*

Submitted 22 October 2012; accepted in final form 26 December 2012

Maison SF, Pyott SJ, Meredith AL, Liberman MC. Olivocochlear suppression of outer hair cells in vivo: evidence for combined action of BK and SK2 channels throughout the cochlea. *J Neurophysiol* 109: 1525–1534, 2013. First published January 2, 2013; doi:10.1152/jn.00924.2012.—Cholinergic inhibition of cochlear hair cells via olivocochlear (OC)-efferent feedback is mediated by Ca^{2+} entry through α_9-/α_{10}-nicotinic receptors, but the nature of the K^+ channels activated by this Ca^{2+} entry has been debated (Yoshida N, Hequembourg SJ, Atencio CA, Rosowski JJ, Liberman MC. *J Neurophysiol* 85: 84–88, 2001). A recent in vitro study (Wersinger E, McLean WJ, Fuchs PA, Pyott SJ. *PLoS One* 5: e13836, 2010) suggests that small-conductance (SK2) channels mediate cholinergic effects in the apical turn, whereas large-conductance (BK) channels mediate basal turn effects. Here, we measure, as a function of cochlear frequency, the magnitude of BK and SK2 expression in outer hair cells and the strength of in vivo OC suppression in $BK^{+/+}$ mice vs. $BK^{-/-}$ lacking the obligatory α-subunit (Meredith AL, Thorneloe KS, Werner ME, Nelson MT, Aldrich RW. *J Biol Chem* 279: 36746–36752, 2004). Except at the extreme apical tip, we see immunostaining for both BK and SK2 in $BK^{+/+}$. Correspondingly, at all testable frequencies (8–45 kHz), we see evidence for both SK2 and BK contributions to OC effects evoked by electrically stimulating the OC bundle: OC-mediated suppression was reduced, but not eliminated, at all frequencies in the $BK^{-/-}$ ears. The suppression remaining in BK nulls was blocked by strychnine, suggesting involvement of α_9-/α_{10}-cholinergic receptors, coupled to activation of the remaining SK2 channels.

inner ear; efferent feedback; calcium-activated channels; cholinergic

BK CHANNELS, THE LARGE-CONDUCTANCE K^+ channels that are cooperatively gated by membrane voltage and Ca^{2+} concentration, are known to be important in sensory transduction in the inner ear (Hafidi et al. 2005; Pyott et al. 2004; Ruttiger et al. 2004; Skinner et al. 2003). In the inner hair cell (IHC), where the great majority of cochlear afferent fibers make synaptic contact, BK channels decrease the membrane time constant, which is key to the rapid onset of IHC receptor potentials in response to stimulus onset and thus to the precise timing of action potentials in the postsynaptic fibers of the cochlear nerve (Oliver et al. 2006). Indeed, the average onset rate of cochlear nerve fibers is reduced by 45% in mice with targeted deletion of the gene for BKα (Oliver et al. 2006), the pore-forming subunit of the BK channel complex (Berkefeld et al. 2010). In the outer hair-cell (OHCs) area, the role of BK channels is subtler. Pharmacological blockade of the BK channel has minimal effect on cochlear microphonic potentials (Skinner et al. 2003), and genetic deletion of the channel has little effect on cochlear thresholds (Pyott et al. 2007), suggesting that the normal contribution of OHC motors to amplification of cochlear mechanical vibrations does not require this conductance. However, recent in vitro work has suggested that BK channels contribute to the inhibitory signaling on OHCs via the medial olivocochlear (MOC)-efferent pathway (Wersinger et al. 2010). ACh released from MOC terminals normally acts on a heteromeric complex of α_9-/α_{10}-ACh receptors in OHCs, increasing Ca^{2+} conductance (Vetter et al. 1999, 2005). The Ca^{2+} entry opens Ca^{2+}-activated K^+ channels, and the resultant K^+ current hyperpolarizes the OHC and reduces its receptor potential (Fuchs and Murrow 1992) and thus its voltage-driven mechanical motors (Dallos 2008).

Evidence for which Ca^{2+}-activated K^+ channels mediate this cholinergic hair-cell inhibition has been contradictory. The in vitro work on isolated hair cells, most of which is from the chick, showed that the cholinergic inhibition was blocked by apamin and concluded that small-conductance (SK2) K^+ channels were involved (Yuhas and Fuchs 1999). However, an in vivo study of MOC-mediated inhibition of cochlear responses in guinea pig showed a lack of apamin sensitivity and concluded that other channels might be involved (Yoshida et al. 2001). A recent reexamination of cholinergic inhibition in rats in vitro suggested a possible resolution of the paradox (Wersinger et al. 2010): i.e., that SK2 channels dominate the cholinergic effects in hair cells from the cochlear apex, where in vitro experiments are easier and thus more commonly done, whereas BK channels dominate the ACh-mediated effects in basal cochlear regions, where in vivo cochlear responses are more informative and thus more commonly studied.

The aim of the present study was to evaluate the frequency dependence in vivo of the role of the BK channel in MOC-mediated inhibition by comparing the magnitude of this efferent effect in BK-channel knockout mice and their wild-type littermates. Results suggest that, in mouse, both BK and SK2 channels make significant contributions to cholinergic inhibition throughout most of the cochlear spiral and that, if there is a region where BK channels are not involved, it is restricted to the apical 20% of the spiral, where in vivo effects are difficult to evaluate.

Address for reprint requests and other correspondence: S. F. Maison, Eaton-Peabody Laboratory, Massachusetts Eye and Ear Infirmary, 243 Charles St., Boston, MA 02114-3096 (e-mail: stephane_maison@meei.harvard.edu).

MATERIALS AND METHODS

Animals and groups. Heterozygous breeding pairs of the mutant mouse line with targeted deletion of the gene for the BKα subunit were obtained from the laboratory of origin (Meredith et al. 2004). The same mutant line has been used in prior studies on the role of BK channels in the inner ear (Pyott et al. 2007). This targeted deletion was created as described elsewhere (Meredith et al. 2004), and the mice were maintained on an FVB/NJ background. Offspring of the heterozygous parental stock were bred and genotyped in-house to produce homozygous null animals and wild-type littermates. For all physiological experiments, animals of either sex were tested at 6 or 15 wk of age. For immunohistochemical studies of the afferent synaptic counts and efferent terminal volumes and BK-SK2 expression patterns, wild-type and knockout ears were evaluated at 6–9 wk. The care and use of the animals was approved by the animal care committee of the Massachusetts Eye and Ear Infirmary.

Cochlear function tests. For measuring cochlear function via auditory brain-stem responses (ABRs) and distortion product otoacoustic emissions (DPOAEs), animals were anesthetized with xylazine (20 mg/kg ip) and ketamine (100 mg/kg ip) and placed in an acoustically electrically shielded room maintained at 32°C. Acoustic stimuli were delivered through a custom EPL Acoustic System consisting of two miniature dynamic earphones used as sound sources (CUI CDMG15008-03A) and an electret condenser microphone (Knowles FG-23329-PO7) coupled to a probe tube to measure sound pressure near the eardrum (for details, see http://www.masseyeandear.org/research/ent/eaton-peabody/epl-engineering-resources/epl-acoustic-system/). Digital stimulus generation and response processing were handled by digital soundboards from National Instruments driven by custom software written in LabVIEW. For ABRs, stimuli were 5-ms tone pips (0.5 ms $\cos^2$ rise-fall) delivered in alternating polarity at 35/s. Electrical responses were sampled via Grass Technologies needle electrodes at the vertex and pinna with a ground reference near the tail and amplified 10,000× with a 300-Hz to 3-kHz band pass. Responses to as many as 1,024 stimuli were averaged at each sound-pressure level (SPL), as level was varied in 5-dB steps from below threshold up to 80-dB SPL. ABR thresholds were defined, by visual inspection of stacked waveforms, as the lowest SPL at which the wave morphology conformed to a consistent pattern (with peak latencies increasing systematically as SPL is reduced). For DPOAEs, stimuli were two primary tones, f_1 and f_2 ($f_2/f_1 = 1.2$), with f_1 level always 10 dB above f_2 level. Primaries were swept in 5-dB steps from 20- to 80-dB SPL (for f_2). The DPOAE at $2f_1$-f_2 was extracted from the ear canal sound pressure after both waveform and spectral averaging. Noise floor was defined as the average of 6 spectral points below and 6 above the $2f_1$-f_2 point. Threshold was computed by interpolation as the primary level (f_2) required to produce a DPOAE of 0-dB SPL.

OC function tests. After anesthetization with urethane (1.20 g/kg ip) and xylazine (20 mg/kg ip), the animal was connected to a respirator via a tracheal cannula. A posterior craniotomy and partial cerebellar aspiration exposed the floor of the fourth ventricle. To stimulate the OC bundle, shocks (monophasic pulses, 150-μs duration, 200/s) were applied through fine silver wires (0.4-mm spacing) placed along the midline, spanning the OC decussation. Shock threshold for facial twitches was determined, and muscle paralysis was induced with α-D-tubocurarine (1.25 mg/kg ip). Shock levels were then raised to 6 dB above twitch threshold. During the OC suppression assay, f_2 level was set to produce a DPOAE 10 dB above the noise floor. To measure OC effects, repeated measures of baseline DPOAE amplitude were first obtained ($n = 54$) followed by a series of 70 contiguous periods in which DPOAE amplitudes were measured with simultaneous shocks to the OC bundle and additional periods during which DPOAE measures continued after the termination of the shock train. During paralysis, heart rate was monitored, and urethane boosters were administered every hour at 25% of the initial dose. To abolish α_9-/α_{10}-mediated OC effects, strychnine was injected (10 mg/kg im) at least 20 min before the OC assay. This concentration completely blocks the suppression of cochlear responses evoked by electrically shocking the OC bundle (Maison et al. 2007b).

Acoustic injury. For studies of acoustic injury, animals were exposed to free-field sound, while awake and unrestrained, in a small reverberant chamber to an 8- to 16-kHz octave band noise presented at 100-dB SPL, for either 15 min or 2 h to create a reversible or irreversible threshold shift, respectively. The exposure stimulus was generated digitally, amplified (Crown power amplifier), and delivered (JBL compression driver) through an exponential horn fitted securely to a hole in the top of a reverberant box. Sound exposure levels were measured at four positions within each cage using a 0.25-in. Brüel & Kjær condenser microphone: sound pressure varied by <0.5 dB across these measurement positions.

Immunohistochemistry. To examine BK channel localization in IHCs, afferent-IHC synapse number, and efferent-OHC synapse morphology, animals were perfused with 4% paraformaldehyde and postfixed for 2 h before removing the temporal bone. The cochlear duct was decalcified in EDTA and then dissected into half-turns of the cochlear spiral. Tissue was incubated in primary antibodies overnight at 37°C, including: rabbit anti-BK (APC-021; 1:500 dilution; Alomone Labs), goat anti-Na^+-K^+-ATPase α_3 (sc-16052; 1:100; Santa Cruz Biotechnology), rabbit anti-vesicular acetylcholine transporter (anti-VAT; V5387; 1:1,000; Sigma), mouse anti-GluA2 (MAB397; 1:2,000; Millipore), or mouse anti-COOH-terminal binding protein 2 (anti-CtBP2; 612044; 1:200; BD Transduction Laboratories). A membrane dye (CellMask; 1:5,000 for 5 min; Invitrogen) was used in some preparations. Secondary incubations were from 1 to 2 h, also at 37°C, using species-appropriate antibodies coupled either to an Alexa Fluor dye or to biotin followed by a streptavidin-coupled Alexa Fluor. When two mouse primaries were used (e.g., CtBP2/GluA2 double-label), the primary isotypes were different, and the secondary antibodies were isotype specific. To quantify BK and SK2 channel expression in the OHC region, fixation was similar, but cochleas were not decalcified, and antibody incubations were performed at room temperature. Primary antibodies were *1*) rabbit anti-SK2 (1:500; gift from Dr. John Adelman), and *2*) either a monoclonal mouse anti-BK (L6/43; 1:500; courtesy of Dr. James Trimmer) or a polyclonal rabbit anti-BK (APC-021; 1:500; Alomone Labs).

Morphometry. Images were acquired at subsaturating laser intensities, using either an Olympus FluoView FV1000 or a Leica SP5. All quantitative image analyses were performed on the raw image stacks, without deconvolution, filtering, or γ-correction. Quantification of the numbers or sizes of afferent or efferent terminals or synaptic puncta was based on either two- or three-dimensional (3-D) analysis of confocal *z*-stacks using Amira (Visualization Sciences Group, Burlington, MA) or Imaris (Bitplane, Saint Paul, MN). To count presynaptic ribbons and postsynaptic glutamate-receptor patches in the IHC area (Fig. 1*C*) or to measure the volume of efferent terminals in the OHC area (Fig. 2), we used the "connected components" feature of Amira software. This tool identifies, in a selected channel of the *z*-stack, all of the clusters of contiguous pixels with intensity greater than a user-set criterion. By comparing a 3-D surface rendering of all of the defined clusters to a (2-D) maximum-projection image, the appropriateness of the criterion can be ascertained, and the volumes of all of the clusters can be exported to a spreadsheet for further analysis. Once a criterion value was selected for each type of analysis, the same criterion was applied to all of the image stacks in that analysis. To determine the volumes of BK and SK2 immunopuncta in the OHC region (Fig. 3*E*), *z*-stacks were analyzed in Imaris. Contour surfaces in the region of interest were made for each channel using a surface area detail of 0.2 μm. Volumes of surfaces (in cubic micrometers) were determined using the statistics option.

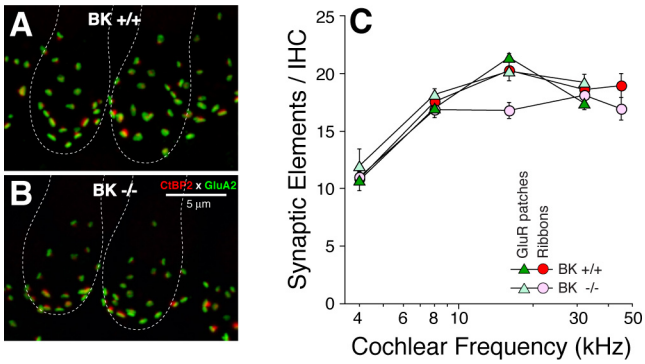

Fig. 1. Cochlear immunostaining shows that inner hair-cell (IHC) synaptic counts in large-conductance $BK^{-/-}$ are similar to $BK^{+/+}$. *A* and *B*: immunostaining for presynaptic ribbons (CtBP2; red) and postsynaptic AMPA-receptor patches (GluA2; green) was used to count synaptic elements. Both images are maximum projections from confocal *z*-stacks in the 16-kHz region. Rough outlines of a pair of adjacent IHCs are shown. *C*: counts of synaptic elements (means ± SE) at 5 cochlear locations. Samples include data from 4 ears of each genotype: at each frequency region, in each ear, 2 adjacent image stacks were acquired, from ~80 IHCs total in each cochlear region, in each genotype. GluR, glutamate receptor.

RESULTS

BK immunolabeling in wild-type cochleas. In adult $BK^{+/+}$ cochleas, BK immunolabeling was seen in both the IHC and OHC areas (Fig. 3). Immunostaining was absent in $BK^{-/-}$ ears (Fig. 3*D*), thus confirming the specificity of the antibody used. In the IHC area (Fig. 3, *A* and *B*), as described in prior reports (Hafidi et al. 2005; Pyott et al. 2004), intense BK immunolabeling was seen in the pericuticular region of the sensory cells, near the hair bundles. As seen in the side-projection of the confocal *z*-stack (Fig. 3*B*), the BK puncta (red) are far from the afferent (blue: Na^+-K^+-ATPase) and efferent (green: synapsin) terminals at the basal pole of the IHC. The images in Fig. 3, *A* and *B*, are from the apical turn, but similar immunostaining was seen throughout the cochlear spiral. In the OHC area, BK- and SK2-positive puncta were seen at the basal pole of the sensory cells (Fig. 3, *C* and *D*). Colabeling with anti-synaptophysin (data not shown) suggested that each of these puncta was located directly opposite an efferent terminal. Except at the extreme apical tip, every synaptophysin-positive efferent terminal was paired with a BK-positive receptor patch. Quantification of puncta volumes as a function of cochlear location suggests that BK expression in the OHC area is stronger in the basal half of the cochlea, whereas SK2 expression is stronger in the apical half (Fig. 3*E*). With respect to radial gradients, BK puncta were slightly larger in the first row than the third row of OHCs (6.8 ± 0.3 vs. 5.3 ± 0.3 μm^3 at the 16-kHz region); differences in SK2 puncta were not significant (9.7 ± 0.7 vs. 9.3 ± 0.7 μm^3 at the 16-kHz region).

Since a number of splice variants of the BK channel α-subunit are expressed in the cochlea (Langer et al. 2003), it is possible that the monoclonal BK channel antibody used for quantification could have to detect one or more variant. To address this, we also examined ears immunostained with a polyclonal BK antibody that should recognize many epitopes: the patterns of immunostaining were qualitatively the same, i.e., there was no BK immunostaining in the extreme apex, and there was a general increase in puncta size from apex to base. The observed lack of BK puncta at the extreme apex is consistent with prior observations that apical-most OHCs lack BK currents in vitro (Wersinger et al. 2010).

From the views in Fig. 3, *C* and *D*, it is difficult to determine whether the BK puncta are located pre- or postsynaptically at these efferent synapses on the OHCs. Using a membrane marker (Fig. 3*G*, cyan) to highlight the circumferential ring of highly elaborated subsurface cisternae within the OHC, the postsynaptic localization of the BK puncta (red arrowheads) is clearly seen, as is also schematized in Fig. 3*F*. The MOC terminals are also visible (cyan arrowhead in Fig. 3*G*) because they are densely packed with the membranes of synaptic vesicles. The Deiters cell cups are often visible because they are packed with mitochondria (white arrows in Fig. 3*G*).

Cochlear afferent innervation and afferent responses in $BK^{-/-}$. As suggested by prior studies of these $BK^{-/-}$ mice (Pyott et al. 2007), cochlear threshold sensitivity is unaffected by the loss of BK channels (Fig. 4). Here, we used two metrics of cochlear function: DPOAEs (Fig. 4*A*) and ABRs (Fig. 4*B*). Both suggest normal OHC function in the $BK^{-/-}$ ears, at 6 and 15 wk of age. Normal DPOAEs require normal OHC function, particularly their contribution to the amplification of mechanical motion in the sensory epithelium (Shera and Guinan 1999); normal ABRs also require normal synaptic function in the IHC area and normal cochlear nerve physiology (Melcher et al. 1996). Although threshold sensitivity was unaffected by the loss of BK channels, the attenuated suprathreshold growth of the cochlear neural responses (Fig. 5, *C* and *D*) and the increased latency of the neural responses (Fig. 5, *E* and *F*) coupled with normal suprathreshold growth of the DPOAEs

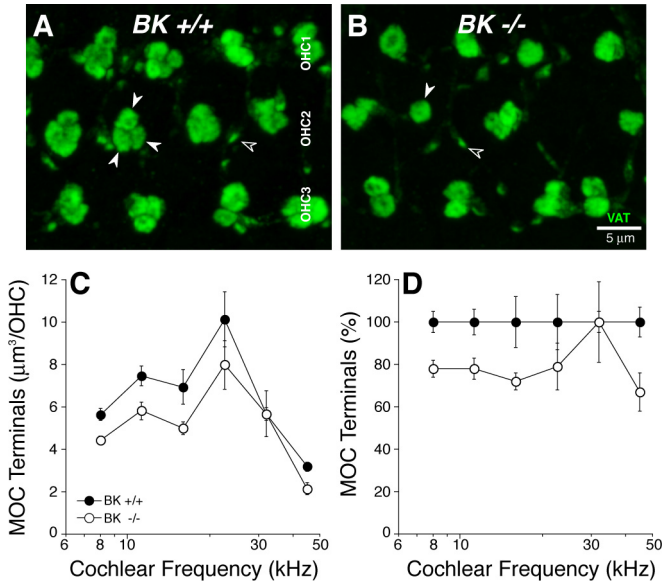

Fig. 2. Immunostaining for a cholinergic marker shows slightly reduced volume of outer hair-cell (OHC)-efferent terminals in $BK^{-/-}$. *A* and *B*: maximum projections of confocal *z*-stacks through the OHC region immunostained with vesicular acetylcholine transporter (VAT; green). Medial olivocochlear (MOC) terminals are normally found in clusters of 2–3 under each OHC, whereas they are often in singlets in $BK^{-/-}$ (closed arrows). The tiny VAT-positive puncta (open arrows) are located well below the OHC bases, within the outer spiral bundles. *C*: mean innervation density (±SE) was quantified by measuring the volume of VAT-positive terminals at 6 locations along the cochlear spiral from $BK^{+/+}$ ($n = 3$) and $BK^{-/-}$ ($n = 3$) ears: in each location, in each ear, 2 image stacks were obtained from contiguous regions, which together spanned 20 OHCs in each row. *D*: data from *C* replotted as the percentage deviation from $BK^{+/+}$ data.

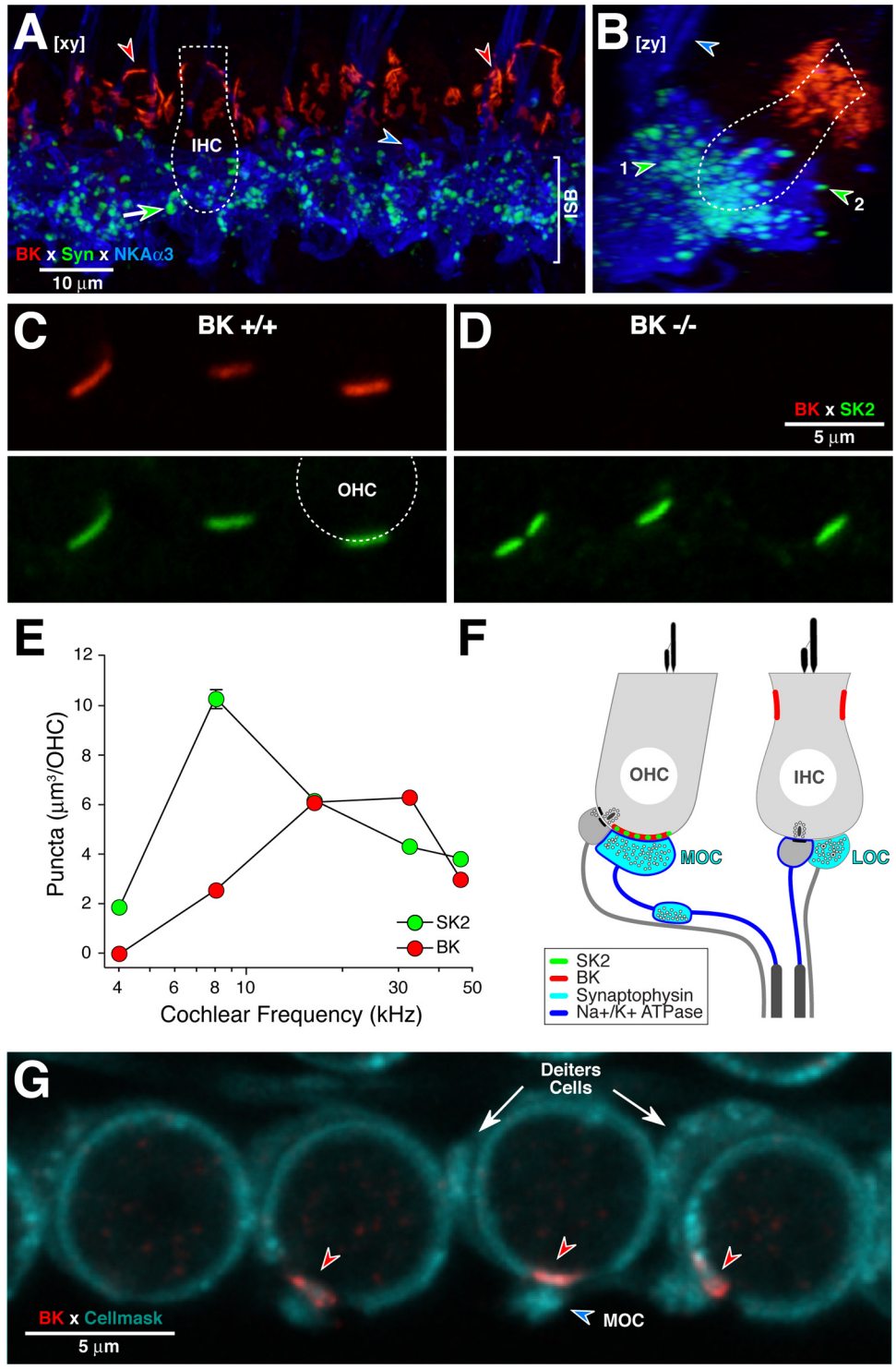

Fig. 3. BK immunolabeling is seen in IHC (*A* and *B*) and OHC (*C* and *D*) areas. *A* and *B*: BK immunostains the IHC near the cuticular plate (red arrowheads), far from the synaptic zone where synaptophysin (Syn)-positive lateral olivocochlear (LOC) terminals (e.g., green-fill arrow) and Na^+-K^+-ATPase-positive afferent terminals (e.g., blue-fill arrowhead in *A*) are located. LOC terminals are seen in the inner spiral bundle (ISB; arrowhead no. 1 in *B*) and close to afferent terminals contacting the IHC (arrowhead no. 2 in *B*). MOC fibers to the OHCs are also immunopositive for Na^+-K^+-ATPase (blue arrowhead in *B*). *A* and *B* are *x*-*y* and *y*-*z* projections, respectively, of a confocal *z*-stack from the 8-kHz region in a $BK^{+/+}$ ear: outline of an IHC (dotted lines) is shown for scale. NKAα3, sodium/potassium-transporting ATPase subunit α3. *C* and *D*: in $BK^{+/+}$ (*C*), BK (red) and small-conductance (SK2; green) colocalize in puncta at the basal poles of OHCs: each paired panel shows the red and green channels in a confocal image (single optical section) from the 16-kHz region. The outline of 1 OHC base is shown (dashed line). In $BK^{-/-}$ ear (*D*), BK immunoreactivity is absent. *E*: quantification of the mean volumes of BK- and SK2-positive immunopuncta at 5 cochlear regions suggests more robust BK expression in the basal half of the cochlea. No BK-positive puncta were observed at the 4-kHz region. For the other frequencies, data are mean volumes (±SE) from 111 to 181 puncta from all 3 OHC rows from 3 to 5 ears per frequency. *F*: schematic of the IHC and OHC areas showing the LOC- and MOC-efferent terminals and the type-I and type-II afferent terminals on IHCs and OHCs, respectively. *G*: BK immunolabeling in the OHC area is postsynaptic. A membrane marker (CellMask; blue-green) labels the OHCs, the Deiters cell cups, and the vesicle-rich efferent terminals. This image of 1st-row OHCs is a maximum projection of 4 consecutive 0.25-μm *z*-slices from the 22-kHz region.

(Fig. 5, *A* and *B*) indicates a deficit in IHC and/or cochlear nerve function and/or in the synaptic transmission between them. Data are shown here only from the 8- and 32-kHz regions; however, a similar response phenotype was present at all other frequencies tested (5.6, 11.3, 16, 22.6, and 45.2 kHz).

Prior studies have shown increased temporal jitter in the onset responses of cochlear nerve fibers in $BK^{-/-}$ ears (Oliver et al. 2006), which would contribute to increased latency and decreased amplitude of ABR wave 1. Nevertheless, to rule out possible synaptopathy in the IHC area as an additional contributing factor, we immunostained cochlear sensory epithelia (Fig. 1, *A* and *B*) for a presynaptic marker (CtBP2; red) and a postsynaptic marker (GluA2; green): the normal one-to-one juxtaposition of presynaptic ribbons and postsynaptic glutamate-receptor patches is present in the $BK^{-/-}$ ears (Fig. 1*B*). Quantification of these paired synaptic elements (Fig. 1*C*) suggests no significant change in the afferent innervation of the IHCs in $BK^{-/-}$ ears.

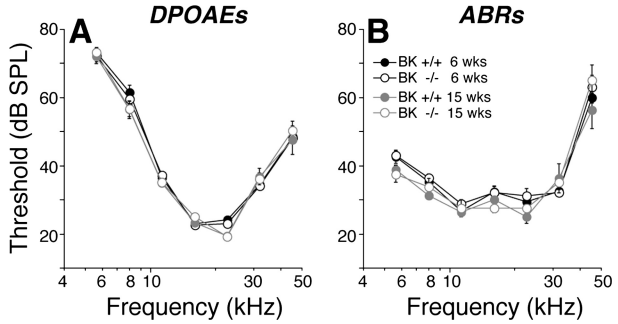

Fig. 4. Cochlear thresholds are normal in $BK^{-/-}$, at both 6 and 15 wk of age, and for both distortion product otoacoustic emissions (DPOAEs; *A*) and auditory brain-stem responses (ABRs; *B*). Means (±SE) are shown; numbers of ears in each DPOAE group were: at 6 wk, 33 $BK^{+/+}$ and 24 $BK^{-/-}$; at 15 wk, 8 $BK^{+/+}$ and 8 $BK^{-/-}$. Key in *B* applies to both panels. SPL, sound-pressure level.

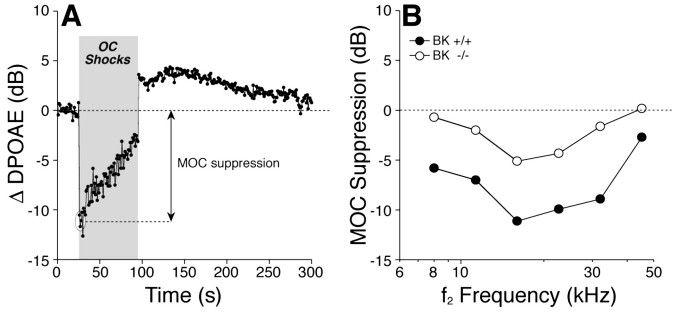

Fig. 6. Efferent effects on OHCs are reduced at all test frequencies in $BK^{-/-}$ ears. *A*: in a sample run of the efferent MOC assay, DPOAEs are measured once per second, before, during, and after a 70-s train of shocks to the OC bundle (gray box). Response amplitudes are normalized to the average of the 25 measurements taken before shock-train onset. The size of MOC suppression is the average normalized DPOAE for the 1st 3 points after shock-train onset (circled). *B*: MOC suppression in $BK^{-/-}$ vs. $BK^{+/+}$ littermates, as a function of stimulus frequency (f_2 is plotted here). For all test frequencies, primary levels are set to evoke a DPOAE 10 dB above the noise floor: typical f_2 levels were ~30 dB at 16 kHz, ~40 dB at 32 kHz, and ~60 dB at 8 kHz. Means from 5 $BK^{+/+}$ and 11 $BK^{-/-}$ ears are shown: SE are smaller than the symbol size.

Cochlear efferent innervation and effects of efferent activation in $BK^{-/-}$. Activation of the OC pathway, in vivo, elicits a complex set of effects, which includes a fast suppression (onset within ~100 ms) and a slow suppression (onset within 1–10 s), both of which are mediated by the α_9-/α_{10}-cholinergic receptor complexes on OHCs (Sridhar et al. 1997) as well as a slow-onset enhancement mediated by a separate (unknown) signaling pathway (Maison et al. 2007b). These effects are demonstrable with our OC assay (Fig. 6*A*) in which DPOAEs evoked by low-level stimuli are measured repeatedly before, during, and after a 70-s shock train to the OC bundle. In the example in Fig. 6*A*, fast suppression is the "immediate" drop in DPOAE amplitude after shock onset: this assay has a time resolution of ~1 s/point, which is too slow to capture the onset time constant of the fast effect. The OC-mediated enhancement is suggested by the postshocks elevation of DPOAE response (Fig. 6*A*). This enhancement is unmasked by blocking the α_9-/α_{10}-cholinergic receptors. Systemic strychnine, a particularly potent α_9-/α_{10}-antagonist (Elgoyhen et al. 2001), removes OC-mediated suppression, leaving a slow-onset, slow-offset DPOAE enhancement that is larger for high-frequency stimuli than for low-frequency stimuli (Fig. 7*A*, thin traces). Similar slow-onset enhancement is seen when the OC bundle is stimulated in mutant mice lacking either α_9-/α_{10}-receptors (Maison et al. 2007b; Fig. 8). The absence of strychnine effects on our OC assay in $\alpha 10^{-/-}$ mutants (Fig. 8) suggests that strychnine has no additional, nonspecific effects on hair-cell physiology.

In $BK^{+/+}$ ears, the magnitude of the fast suppression is maximal for midfrequency tones and falls off at higher and lower frequencies (Fig. 6*B*), mirroring the density of OC innervation along the cochlear spiral (Maison et al. 2003). Fast suppression is dramatically reduced in $BK^{-/-}$ ears for all test frequencies (Fig. 6*B*). Assuming that SK2 and BK are the only K^+ channels mediating the downstream effects of Ca^{2+} entry through α_9-/α_{10}-cholinergic receptors, we can estimate the contributions of SK2 channels at different cochlear locations by comparing OC-mediated suppression in $BK^{-/-}$ ears with vs. without strychnine. The result (blue traces in Fig. 7*B*) suggests that SK2 makes a smaller contribution to OC-mediated suppression in the cochlear apex than in the base. Similarly, we can estimate the magnitude of BK-mediated contributions to α_9/α_{10} effects by taking the difference between OC

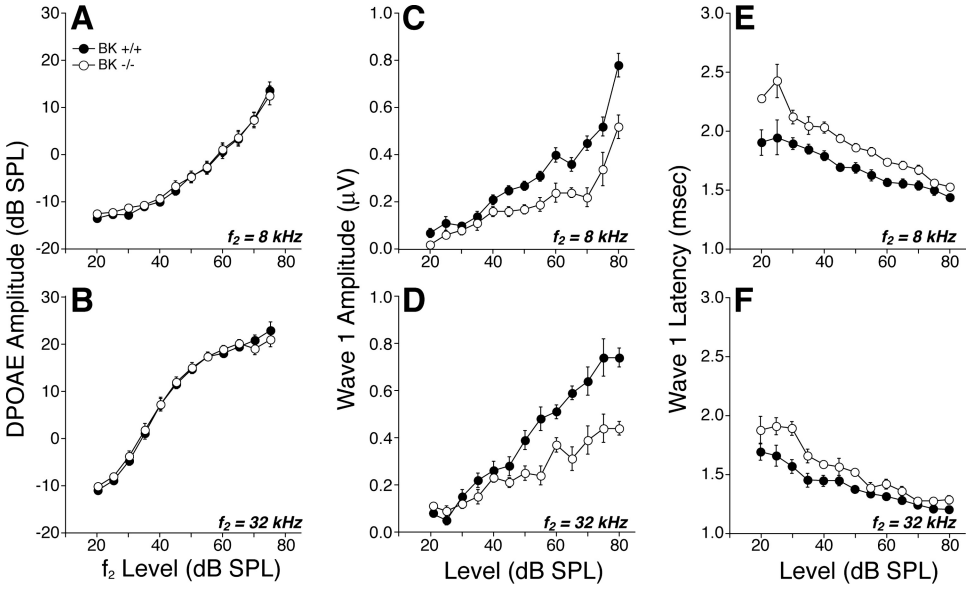

Fig. 5. Suprathreshold DPOAE responses (*A* and *B*) are normal in $BK^{-/-}$; however, ABR wave-1 amplitudes (*C* and *D*) and the summed responses of the cochlear nerve fibers are reduced, and their latencies (*E* and *F*) are prolonged. Mean data (±SE) are shown; group sizes are the same as in Fig. 4. Key in *A* applies to all panels. Data were obtained at age 6 wk.

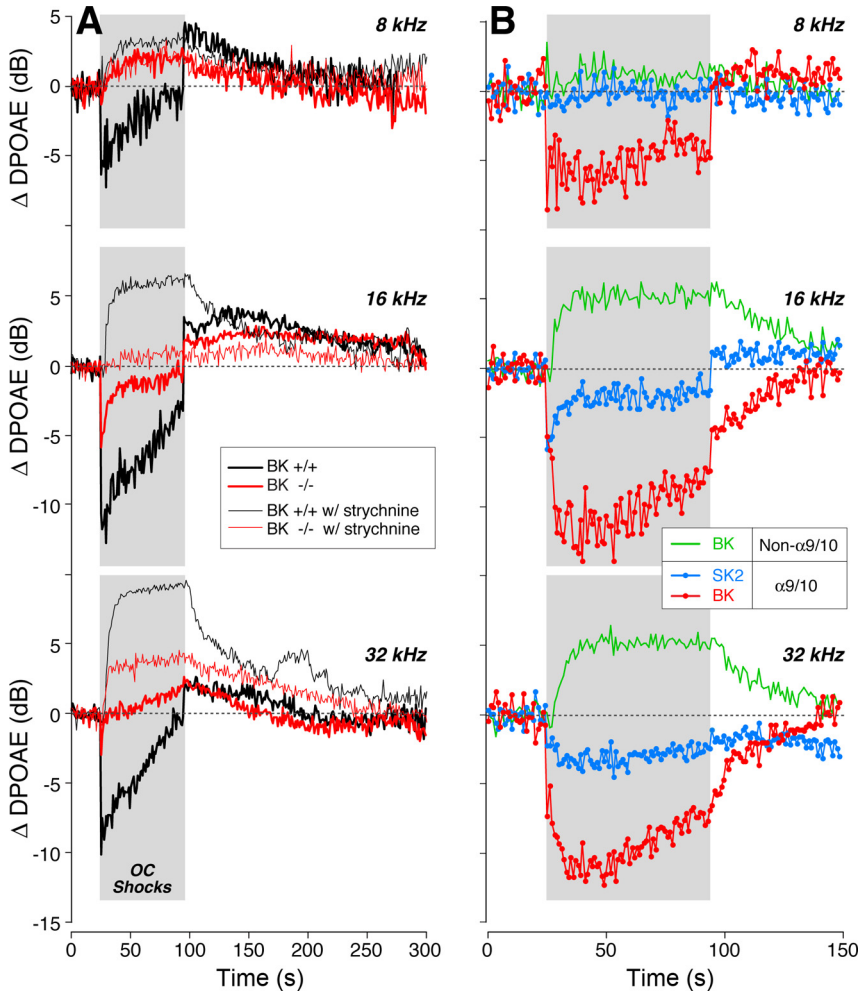

Fig. 7. Strychnine blockade of MOC-elicited effects in $BK^{-/-}$ vs. $BK^{+/+}$ suggests BK channels are key contributors to fast and slow suppressive effects as well as the strychnine-insensitive enhancement. *A*: average effects of MOC shocks on DPOAE amplitudes evoked at 3 f_2 frequencies (8, 16, or 32 kHz, as indicated) from 11 $BK^{-/-}$ and 5 $BK^{+/+}$ ears, as measured either with (thin trace) or without (thick trace) strychnine blockade of effects mediated by the α_9-/α_{10}-ACh receptors. *B*: contributions of SK2 channels and BK channels to (α_9-/α_{10}-mediated) suppression and (non-α_9-/α_{10}-mediated) enhancement are derived by mathematically combining traces from column *A*: SK2-mediated suppression (blue) = $BK^{-/-}$ − $BK^{-/-}$ with strychnine; BK-mediated enhancement (green) = $BK^{+/+}$ with strychnine − $BK^{-/-}$ with strychnine; BK-mediated suppression (red) = $BK^{+/+}$ − $BK^{-/-}$ − $BK^{+/+}$ with strychnine − $BK^{-/-}$ with strychnine. Gray box in each panel shows duration of shock train. DPOAE amplitudes are normalized before averaging as described in Fig. 6.

effects in $BK^{+/+}$ and $BK^{-/-}$ ears after removing any BK-mediated effects that are not coupled to α_9/α_{10} complexes (see caption to Fig. 7). The result (red traces in Fig. 7*B*) suggests a robust contribution of BK channels to OC-mediated suppression throughout the cochlear spiral but largest in the basal turn. To evaluate the role of BK channels in the slower effects of OC activation, we block α_9/α_{10} effects with strychnine and then compare the OC-mediated changes in $BK^{+/+}$ vs. $BK^{-/-}$ ears. The result (green traces in Fig. 7*B*) suggests that the BK channels are also a major contributor to OC-mediated enhancement.

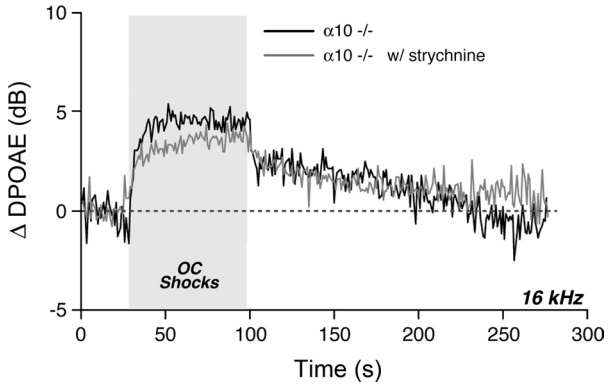

Fig. 8. Strychnine has no effect on the slow enhancement of cochlear responses evoked by shocking the OC bundle in α_{10}-null mice. These data are mean responses from 3 runs performed before strychnine injection (black) and 5 runs performed after (w/) strychnine injection (gray) in 1 animal.

Given prior reports of dysmorphology and/or degeneration of efferent terminals in mouse mutants lacking SK2 channels (Murthy et al. 2009) or either of the OHC ACh receptors, α_9 (Vetter et al. 1999) or α_{10} (Vetter et al. 2005), it is possible that the attenuation of OC effects in $BK^{-/-}$ ears arises from a reduction in the density of efferent innervation. To test this, we immunostained cochleas (Fig. 2, *A* and *B*) for VAT, a robust marker of the cytoplasm of OC peripheral terminals (Maison et al. 2003), and for the Na^+-K^+-ATPase that is present in the membranes of efferent fibers in the OHC area (McLean et al. 2009). As shown in Fig. 2, *C* and *D*, quantification revealed a slight reduction in efferent terminal density all along the cochlear spiral. This dysmorphology of the efferent innervation, which appears significant only in the apical half of the cochlea, cannot fully explain the reduction in the strength of OC-mediated fast suppression in the $BK^{-/-}$ ears, which was seen at all test frequencies (Fig. 6*B*).

Vulnerability to acoustic injury in $BK^{-/-}$. The efferent fibers to OHCs comprise a sound-evoked negative feedback loop that limits the growth of cochlear responses with increasing SPL and thereby minimizes the damage from acoustic overstimulation (Maison and Liberman 2000). The overall reduction in shock-evoked OC effects in the $BK^{-/-}$ ears described above (Fig. 6*B*) suggests that $BK^{-/-}$ animals should be more vulner-

able to acoustic injury. To test this idea, we exposed groups of $BK^{+/+}$ and $BK^{-/-}$ animals to two types of overstimulation: one designed to produce only a temporary threshold shift (Fig. 9, *A* and *B*; octave-band noise at 94-dB SPL for 2 h) and one designed to produce a permanent threshold shift (Fig. 9, *C* and *D*; the same octave-band noise at 100-dB SPL for 2 h). As seen in Fig. 9, the $BK^{-/-}$ animals were significantly more vulnerable to the temporary threshold shift but not the permanent threshold shift.

DISCUSSION

BK channel expression in the mammalian cochlea. The BK channel consists of a tetrameric assembly of pore-forming, obligatory α-subunits coupled to several types of modulatory β-subunits (Berkefeld et al. 2010). Immunostaining in the adult ear shows that BK channels are most robustly expressed in the pericuticular region of IHCs (Hafidi et al. 2005; Pyott et al. 2004; Fig. 3) throughout the cochlear spiral from apex to base. An in situ hybridization study (Langer et al. 2003) also reported consistently stronger labeling of IHCs than OHCs and no tonotopic differences in transcript expression. Although there are reports that BK channels are also expressed in spiral ganglion neurons (Skinner et al. 2003), we saw no evidence for channels localized to the afferent terminals in the IHC area in the adult ear (Fig. 3). In the developing ear, BK channels are transiently expressed in efferent terminals synapsing on the IHCs (Zorrilla de San Martin et al. 2010). Our data are consistent with the idea that this expression does not continue into adulthood.

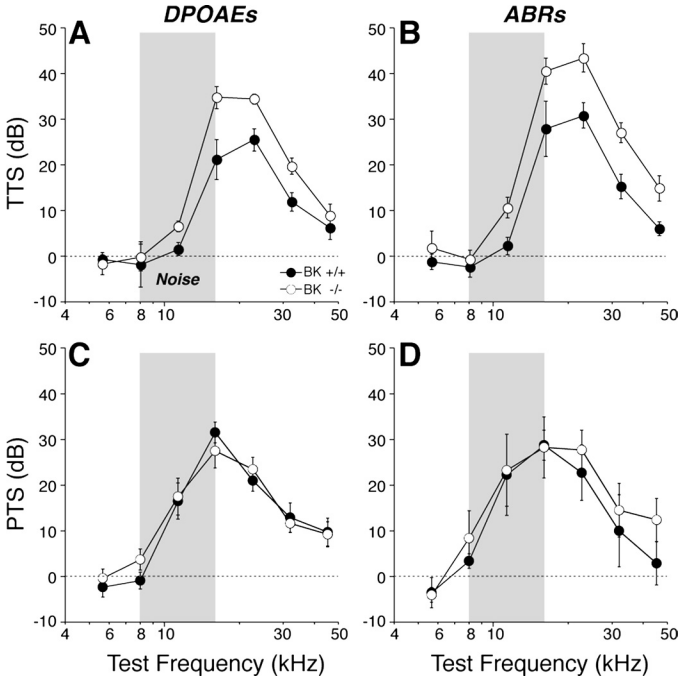

Fig. 9. $BK^{-/-}$ mice are more vulnerable to temporary noise-induced hearing loss (*A* and *B*) but not to permanent noise-induced hearing loss (*C* and *D*), as measured by both DPOAEs (*A* and *C*) and ABRs (*B* and *D*). For temporary threshold shift (TTS), mice were exposed to the 8- to 16-kHz octave band at 94 dB for 15 min and tested 6 h later. Means (±SE) are shown; numbers of ears in each group were: DPOAE, 12 $BK^{+/+}$ and 12 $BK^{-/-}$; ABR, 6 $BK^{+/+}$ and 6 $BK^{-/-}$. For permanent threshold shift (PTS), mice were exposed to the 8- to 16-kHz octave band at 100-dB SPL for 2 h and tested 1 wk later. Means (±SE) are shown; numbers of ears in each group were: DPOAE, 10 $BK^{+/+}$ and 10 $BK^{-/-}$; ABR, 5 $BK^{+/+}$ and 5 $BK^{-/-}$.

In the OHC area of the adult ear, we saw BK puncta opposite all OHC-efferent terminals outside of the most apical cochlear region. BK channels were expressed at the interface between presynaptic OC-efferent terminals and the postsynaptic OHC membrane (Engel et al. 2006; Hafidi et al. 2005; Wersinger et al. 2010; Fig. 3). At the light-microscopic level, it is difficult to distinguish pre- from postsynaptic label at these synapses. Although the images presented here (Fig. 3*G*) suggest a postsynaptic localization, a prior electron microscopic study, using a different antibody, presented images suggesting both pre- and postsynaptic localization at OHC-efferent synapses in the adult mouse (Sakai et al. 2011).

Given the putative presence of BK channels, at varying points in development, in both hair-cell types and in both afferent and efferent fibers of the inner ear, the constitutive deletion of BKα subunits could affect cochlear function via multiple mechanisms. When present in efferent terminals, the BK channel limits the duration of the depolarizing pulse evoked by the invading action potential (Zorrilla de San Martin et al. 2010). Thus the knockout phenotype should be characterized by an increase in efferent effects, which is not what we observed (Fig. 6). In contrast, BK channels on the postsynaptic side are putatively involved in the hair-cell K^+ current that underlies efferent suppression (Wersinger et al. 2010). Thus the knockout phenotype should be characterized by a reduced efferent effect, as was indeed observed (Fig. 6).

BK effects in the IHC area: ABR thresholds vs. ABR amplitudes. Prior loss-of-function studies of BK channels have used two independently derived mutant lines with targeted deletion of KCNMA1, the gene coding for the obligatory α-subunit (Meredith et al. 2004; Sausbier et al. 2004). Both of these lines show normal cochlear thresholds when measured at ages <8 wk. However, one of these knockout lines (Sausbier et al. 2004) shows a prominent progressive high-frequency hearing loss with threshold elevations of 20–30 dB by 16 wk of age. In contrast, the other knockout line (Meredith et al. 2004) showed no threshold shift at 12 wk in a prior study (Pyott et al. 2007) and showed no threshold shifts out to 15 wk in the present study (Fig. 4*B*). The most likely reason for this discrepancy is the difference in genetic background. The knockout examined by Ruttiger et al. (2004) was maintained in a 129/SvJ background, whereas the knockout examined by Pyott et al. (2007) was maintained in an FVB/N background. The BK deletion may interact with the preexisting anomalies in the 129/SvJ line that predispose the ear in that strain to degenerate prematurely (Yoshida et al. 2000).

In the present study, we showed that, although cochlear thresholds were unaffected by the loss of BK channels, as previously reported (Pyott et al. 2007), the amplitudes of the cochlear neural responses were reduced (Fig. 5, *C* and *D*; also see Skinner et al. 2003), and the latencies were prolonged (Fig. 5, *E* and *F*). The reduced growth of the ABR amplitudes is quantitatively similar to the reductions in sound-evoked discharge rates seen in single auditory-nerve fibers in a prior study examining $BK^{-/-}$ mice maintained on the 129/SvJ background (Sausbier et al. 2004). For example, the ABR responses measured here, in particular the amplitudes of wave 1, the summed activity of auditory-nerve fibers, were reduced on average to ~60% of normal by the BK deletion (means of 60- to 80-dB

SPL at 32 kHz; Fig. 5*D*). Correspondingly, the peak discharge rates measured in single auditory-nerve fibers were reduced to 55% of normal according to the prior study (Oliver et al. 2006). These fractional reductions in auditory-nerve response have minimal effect on ABR thresholds because single-fiber spikes add linearly to the amplitudes of gross potentials like the ABR and because, near threshold, additional fibers are recruited so rapidly with SPL that only a few decibels increase is required to compensate for a 40% reduction in discharge rates (see Lin et al. 2011 for more detailed discussion).

The normal growth of DPOAE amplitudes (Fig. 5, *A* and *B*) in the absence of BK channels suggests that these response attenuations do not arise in cochlear mechanics, mechanoelectrical transduction, or OHC-based cochlear amplification (Shera and Guinan 1999). The normal morphology of the cochlear nerve terminals and the normal synaptic counts in the IHC area (Fig. 1) suggest that aberrant development or frank neuropathy of the auditory nerve is also not the underlying problem. The decreases in sound-evoked discharge rates of auditory-nerve fibers, particularly in the peak rates seen at stimulus onset (Oliver et al. 2006), which dominate ABR responses to short-tone pips, are well-explained by the slowing of the receptor potentials due to increased membrane time constants from loss of the BK channels in IHCs (Oliver et al. 2006). This slowing of the receptor potential increases the variance of the first-spike latency, decreasing the synchronization of auditory-nerve responses, which decreases ABR wave 1 and increases its latency.

BK effects in the OHC area: efferent neurotransmission vs. efferent development. In vitro hair-cell studies have long suggested that suppressive effects of efferent terminals are mediated by a two-step process in which ACh-gated Ca^{2+} entry through the hair-cell α_9-/α_{10}-receptors activates SK2 channels and a subsequent K^+ current, which hyperpolarizes the hair cells and reduces their receptor potentials (for review, see Guinan 2006). However, a recent rat study suggested that the SK2 role in efferent effects was limited to apical hair cells, where in vitro work had concentrated in the past, and that BK was the key K^+ channel for basal-turn hair cells (Wersinger et al. 2010): more specifically, apical cells in the Wersinger et al. (2010) study were isolated from locations 92–85% of the distance from base to apex, whereas basal cells were from the 35–25% locus.

The present study, examining the in vivo consequences of BK deletion, suggests that BK channels play a key role in efferent function along most of the cochlear spiral (Fig. 6*B*), i.e., at least from 8 to 45 kHz, which, in mouse, corresponds to locations from 81 to 22% of the distance from base to apex (Taberner and Liberman 2005). Although this diminution of OC-mediated suppression could arise from decreased expression of ACh receptors or SK2 channels elicited by the BK deletion, a microarray study of these BK-null ears suggests that this is not the case (Pyott et al. 2007).

The observation that the size of the efferent terminals is reduced throughout the cochlear spiral in the $BK^{-/-}$ ears (Fig. 2) suggests that the diminished magnitude of OC-mediated suppression could be partly due to a failure of normal efferent development in the absence of BK channels. The apparent contribution of BK channels to OC-mediated enhancement (green traces in Fig. 7*B*) may also arise, in part, from the reduction in efferent terminal size: the BK contribution is derived by comparing the (large) OC-mediated enhancement in wild-types under strychnine blockade to the (small) enhancement seen in strychnine-treated $BK^{-/-}$ ears (thin traces in Fig. 7*A*). The reduction in efferent terminal size in the $BK^{-/-}$ ears may reduce the magnitudes of both the fast suppression and the slow enhancement that OC activation elicits.

Moderate dysmorphology of efferent terminals has been observed in the α_9 (Vetter et al. 1999) and the α_{10} (Vetter et al. 2007) knockout mice, and, in the SK2 knockout, the OHC efferents are largely absent in the adult ear (Murthy et al. 2009). Thus normal signaling at this cholinergic synapse is clearly necessary for the development and/or maintenance of these efferent terminals.

In the present study, we found no evidence for an apical cochlear region where BK channels are not involved in OC-mediated effects, as suggested by the in vitro study (Wersinger et al. 2010). We saw clear-cut reduction in mean OC-mediated suppression in the $BK^{-/-}$ ears at the lowest frequency tested (Fig. 6*B*, 8-kHz point). We also saw minimal effect of strychnine-blockade on OC effects in the $BK^{-/-}$ ears at this low-frequency point (Fig. 8*B*, 8-kHz blue trace), suggesting a minimal role for SK2 channels in OC effects in the apical turn. Both implications of the in vivo results appear to contradict the in vitro pharmacological results (Wersinger et al. 2010). This apparent contradiction may arise because mouse is different from rat, because hair cells at P21, as studied in vitro, are not fully mature, or because our lowest DPOAE-evoking tone pair was too high: in mouse, the 90% cochlear locus corresponds to a frequency of ~5.4 kHz. Our immunolabeling data show colocalization of both BK and SK2 at the OC synapses in the 8-kHz region but indeed suggest that BK effects might be smaller at the very apical tip of the cochlea (Fig. 3*E*). Unfortunately, DPOAEs cannot be evoked reliably in this mouse strain at such low frequencies (Fig. 4*A*).

The present study is also inconsistent with the suggestion from the rat in vitro work (Wersinger et al. 2010) that SK2 channels are uninvolved in efferent transmission in basal-turn hair cells. We saw SK2 expression throughout the basal turn, at least as far as the 45-kHz locus (22% from the base: Fig. 3*E*). When we measured OC effects in the $BK^{-/-}$ ears and then added strychnine to block the α_9-/α_{10}-ACh receptor complexes, we saw changes in the OHC responses (blue traces in Fig. 8*B*) suggesting there was significant OC-mediated suppression remaining in the $BK^{-/-}$ ears. Given that the same strychnine dose had no effect on OC-mediated modulation of OHC responses in a mutant mouse lacking the α_9-/α_{10}-ACh receptor complexes (Fig. 7), the data provide strong evidence for the presence of another functional calcium-activated K^+ channel at the efferent synapses throughout the basal turn. Presently, SK2 is the most reasonable candidate. Thus, although hair cells at the apical-most tip of the sensory epithelium may have different expression of calcium-activated K^+ channels that provides important insight into the gradients that drive cochlear development, this difference in the adult ear is so restricted in spiral extent that it may have limited functional significance.

Activation of efferent terminals on OHCs in vivo is driven by a sound-evoked reflex that reduces cochlear damage at high sound levels (Maison and Liberman 2000). Although overexpression of α_9-ACh receptors enhances OC effects, when measured by the same assay used here (Fig. 6), and also

reduces both temporary and permanent acoustic injury (Maison et al. 2002), overexpression of SK2 channels does not alter susceptibility to permanent noise damage despite the fact that it also enhances OC effects measured via our OC assay (Maison et al. 2007a). Correspondingly, we show here that BK channel deletion does not enhance vulnerability to permanent noise damage (Fig. 9, *C* and *D*) despite the fact that it reduces OC effects measured as shock-evoked suppression of DPOAEs (Fig. 6*B*). These results suggest that resistance to permanent acoustic injury is mediated by downstream effects of Ca^{2+} entry through α_9-/α_{10}-receptors beyond the activation of K^+ channels. As discussed elsewhere, such additional effects could include protein phosphorylation, or other structural modifications, that alter the sound-evoked mechanical motions of the cochlear partition at high sound pressures (Maison et al. 2007a). It is not clear why BK deletion should enhance vulnerability to temporary threshold shift despite its lack of effect on permanent threshold shifts; however, it is not paradoxical given that the functionally important structural modifications underlying temporary vs. permanent noise damage are fundamentally different (Wang et al. 2002).

ACKNOWLEDGMENTS

Flawless technical support in the preparation and immunostaining of cochlear whole mounts by Leslie Liberman is gratefully acknowledged.

GRANTS

This work was supported by grants from the Hearing Health Foundation (S. J. Pyott) and the National Institutes of Health Grants R01-DC-0188 (M. C. Liberman), P30-DC-5029 (M. C. Liberman), and R01-HL-102758 (A. L. Meredith).

DISCLOSURES

No conflicts of interest, financial or otherwise, are declared by the author(s).

AUTHOR CONTRIBUTIONS

S.F.M. and M.C.L. conception and design of research; S.F.M., S.J.P., and M.C.L. performed experiments; S.F.M., S.J.P., and M.C.L. analyzed data; S.F.M. and M.C.L. interpreted results of experiments; S.F.M., S.J.P., and M.C.L. prepared figures; S.F.M. and M.C.L. drafted manuscript; S.F.M., S.J.P., A.L.M., and M.C.L. edited and revised manuscript; S.F.M., S.J.P., A.L.M., and M.C.L. approved final version of manuscript.

REFERENCES

Berkefeld H, Fakler B, Schulte U. Ca^{2+}-activated K^+ channels: from protein complexes to function. *Physiol Rev* 90: 1437–1459, 2010.

Dallos P. Cochlear amplification, outer hair cells and prestin. *Curr Opin Neurobiol* 18: 370–376, 2008.

Elgoyhen AB, Vetter DE, Katz E, Rothlin CV, Heinemann SF, Boulter J. α10: A determinant of nicotinic cholinergic receptor function in mammalian vestibular and cochlear mechanosensory hair cells. *Proc Natl Acad Sci USA* 98: 3501–3506, 2001.

Engel J, Braig C, Ruttiger L, Kuhn S, Zimmermann U, Blin N, Sausbier M, Kalbacher H, Munkner S, Rohbock K, Ruth P, Winter H, Knipper M. Two classes of outer hair cells along the tonotopic axis of the cochlea. *Neuroscience* 143: 837–849, 2006.

Fuchs PA, Murrow BW. Cholinergic inhibition of short (outer) hair cells of the chick's cochlea. *J Neurosci* 12: 800–809, 1992.

Guinan JJ Jr. Olivocochlear efferents: anatomy, physiology, function, and the measurement of efferent effects in humans. *Ear Hear* 27: 589–607, 2006.

Hafidi A, Beurg M, Dulon D. Localization and developmental expression of BK channels in mammalian cochlear hair cells. *Neuroscience* 130: 475–484, 2005.

Langer P, Grunder S, Rusch A. Expression of Ca^{2+}-activated BK channel mRNA and its splice variants in the rat cochlea. *J Comp Neurol* 455: 198–209, 2003.

Lin HW, Furman AC, Kujawa SG, Liberman MC. Primary neural degeneration in the Guinea pig cochlea after reversible noise-induced threshold shift. *J Assoc Res Otolaryngol* 12: 605–616, 2011.

Maison SF, Adams JC, Liberman MC. Olivocochlear innervation in mouse: immunocytochemical maps, crossed vs. uncrossed contributions and colocalization of ACh, GABA, and CGRP. *J Comp Neurol* 455: 406–416, 2003.

Maison SF, Liberman MC. Predicting vulnerability to acoustic injury with a non-invasive assay of olivocochlear reflex strength. *J Neurosci* 20: 4701–4707, 2000.

Maison SF, Luebke AE, Liberman MC, Zuo J. Efferent protection from acoustic injury is mediated via alpha9 nicotinic acetylcholine receptors on outer hair cells. *J Neurosci* 22: 10838–10846, 2002.

Maison SF, Parker LL, Young L, Adelman JP, Zuo J, Liberman MC. Overexpression of SK2 channels enhances efferent suppression of cochlear responses without enhancing noise resistance. *J Neurophysiol* 97: 2930–2936, 2007a.

Maison SF, Vetter DE, Liberman MC. A novel effect of cochlear efferents: in vivo response enhancement does not require α9 cholinergic receptors. *J Neurophysiol* 97: 3269–3278, 2007b.

McLean WJ, Smith KA, Glowatzki E, Pyott SJ. Distribution of the Na,K-ATPase alpha subunit in the rat spiral ganglion and organ of Corti. *J Assoc Res Otolaryngol* 10: 37–49, 2009.

Melcher JR, Knudson IM, Fullerton BC, Guinan JJ Jr, Norris BE, Kiang NY. Generators of the brainstem auditory evoked potential in cat. I. An experimental approach to their identification. *Hear Res* 93: 1–27, 1996.

Meredith AL, Thorneloe KS, Werner ME, Nelson MT, Aldrich RW. Overactive bladder and incontinence in the absence of the BK large conductance Ca^{2+}-activated K^+ channel. *J Biol Chem* 279: 36746–36752, 2004.

Murthy V, Maison SF, Taranda J, Haque N, Bond CT, Elgoyhen AB, Adelman JP, Liberman MC, Vetter DE. SK2 channels are required for function and long-term survival of efferent synapses on mammalian outer hair cells. *Mol Cell Neurosci* 40: 39–49, 2009.

Oliver D, Taberner AM, Thurm H, Sausbier M, Arntz C, Ruth P, Fakler B, Liberman MC. The role of BKCa channels in electrical signal encoding in the mammalian auditory periphery. *J Neurosci* 26: 6181–6189, 2006.

Pyott SJ, Glowatzki E, Trimmer JS, Aldrich RW. Extrasynaptic localization of inactivating calcium-activated potassium channels in mouse inner hair cells. *J Neurosci* 24: 9469–9474, 2004.

Pyott SJ, Meredith AL, Fodor AA, Vazquez AE, Yamoah EN, Aldrich RW. Cochlear function in mice lacking the BK channel alpha, beta1, or beta4 subunits. *J Biol Chem* 282: 3312–3324, 2007.

Ruttiger L, Sausbier M, Zimmermann U, Winter H, Braig C, Engel J, Knirsch M, Arntz C, Langer P, Hirt B, Muller M, Kopschall I, Pfister M, Munkner S, Rohbock K, Pfaff I, Rusch A, Ruth P, Knipper M. Deletion of the Ca^{2+}-activated potassium (BK) alpha-subunit but not the BKbeta1-subunit leads to progressive hearing loss. *Proc Natl Acad Sci USA* 101: 12922–12927, 2004.

Sakai Y, Harvey M, Sokolowski B. Identification and quantification of full-length BK channel variants in the developing mouse cochlea. *J Neurosci Res* 89: 1747–1760, 2011.

Sausbier M, Hu H, Arntz C, Feil S, Kamm S, Adelsberger H, Sausbier U, Sailer CA, Feil R, Hofmann F, Korth M, Shipston MJ, Knaus HG, Wolfer DP, Pedroarena CM, Storm JF, Ruth P. Cerebellar ataxia and Purkinje cell dysfunction caused by Ca^{2+}-activated K^+ channel deficiency. *Proc Natl Acad Sci USA* 101: 9474–9478, 2004.

Shera CA, Guinan JJ Jr. Evoked otoacoustic emissions arise by two fundamentally different mechanisms: a taxonomy for mammalian OAEs. *J Acoust Soc Am* 105: 782–798, 1999.

Skinner LJ, Enee V, Beurg M, Jung HH, Ryan AF, Hafidi A, Aran JM, Dulon D. Contribution of BK Ca^{2+}-activated K^+ channels to auditory neurotransmission in the Guinea pig cochlea. *J Neurophysiol* 90: 320–332, 2003.

Sridhar TS, Brown MC, Sewell WF. Unique postsynaptic signaling at the hair cell efferent synapse permits calcium to evoke changes on two time scales. *J Neurosci* 17: 428–437, 1997.

Taberner AM, Liberman MC. Response properties of single auditory nerve fibers in the mouse. *J Neurophysiol* 93: 557–569, 2005.

Vetter DE, Katz E, Maison SF, Taranda J, Huang C, Elgoyhen AB, Liberman MC, Boulter J. Role of α10 nAChR subunits in the development and function of the olivocochlear system. *Abstracts of the XXVIIIth ARO Midwinter Meeting* 28: 2005.

Vetter DE, Katz E, Maison SF, Taranda J, Turcan S, Ballestero J, Liberman MC, Elgoyhen AB, Boulter J. The alpha10 nicotinic acetylcholine receptor subunit is required for normal synaptic function and integrity of the olivocochlear system. *Proc Natl Acad Sci USA* 104: 20594–20599, 2007.

Vetter DE, Liberman MC, Mann J, Barhanin J, Boulter J, Brown MC, Saffiote-Kolman J, Heinemann SF, Elgoyhen AB. Role of alpha9 nicotinic ACh receptor subunits in the development and function of cochlear efferent innervation. *Neuron* 23: 93–103, 1999.

Wang Y, Hirose K, Liberman MC. Dynamics of noise-induced cellular injury and repair in the mouse cochlea. *J Assoc Res Otolaryngol* 3: 248–268, 2002.

Wersinger E, McLean WJ, Fuchs PA, Pyott SJ. BK channels mediate cholinergic inhibition of high frequency cochlear hair cells. *PLoS One* 5: e13836, 2010.

Yoshida N, Hequembourg SJ, Atencio CA, Rosowski JJ, Liberman MC. Acoustic injury in mice: 129/SvEv is exceptionally resistant to noise-induced hearing loss. *Hear Res* 141: 97–106, 2000.

Yoshida N, Liberman MC, Brown MC, Sewell WF. Fast, but not slow, effects of olivocochlear activation are resistant to apamin. *J Neurophysiol* 85: 84–88, 2001.

Yuhas WA, Fuchs PA. Apamin-sensitive, small-conductance, calcium-activated potassium channels mediate cholinergic inhibition of chick auditory hair cells. *J Comp Physiol A* 185: 455–462, 1999.

Zorrilla de San Martin J, Pyott S, Ballestero J, Katz E. $Ca^{(2+)}$ and $Ca^{(2+)}$-activated $K^{(+)}$ channels that support and modulate transmitter release at the olivocochlear efferent-inner hair cell synapse. *J Neurosci* 30: 12157–12167, 2010.